

## Investigating effects from restricted diffusion in multi-component diffusion data

*Tina Pavlin<sup>1</sup> and John Georg Seland<sup>2</sup>*

<sup>1</sup> Department of Biomedicine, University of Bergen, Norway

<sup>2</sup> Department of Chemistry, University of Bergen, Norway

Corresponding author: John Georg Seland, Dept. of Chemistry, University of Bergen, NO-5007, Bergen, Norway, E-Mail: John.Seland@kj.uib.no

### Abstract

We have investigated model systems in which effects from non-Gaussian restricted diffusion could be separated from effects caused by multiple diffusion coefficients. We applied various models to analyze the experimental data. An analysis based on multi-exponential models does not account correctly for effects caused by restricted diffusion in a system with multiple compartments. However, separating the components due to differences in dynamic behavior prior to the diffusion analysis, combined with a diffusion analysis based on the second cumulant approximation, was more robust, and was able to handle effects from restricted diffusion in the presence of multi-component diffusion.

### Keywords

NMR, heterogeneous systems, diffusion, multiple components, relaxation.

### 1. Introduction

Heterogeneous systems are encountered in NMR applications both in petrophysics and in biomedical MRI. In such systems, multiple diffusion coefficients can be detected, which potentially can be assigned to different diffusion domains or compartments. One method of extracting geometrical information is to apply multi-exponential models to the obtained diffusion attenuated signal, resulting in a measurement of multiple diffusion coefficients, which are then attributed to multiple diffusion domains. However, in order to reach sufficient signal decay for the slow diffusion components, a multi-exponential model necessitates the use of relatively high values of the gradient wave number  $q$ . This will make restricted diffusion a non-Gaussian process [1-4], which can no longer be modeled using mono-exponential models [1,5]. In this work we investigated model systems where effects from non-Gaussian restricted diffusion can be separated from effects caused by multiple diffusion domains.

## 2. Materials and Methods

### 2.1. Samples and Experimental Details

Water molecules confined in a sample of close-packed mono-sized compact spheres display a single-compartment diffusion, but are strongly influenced by non-Gaussian restricted diffusion [5]. Therefore, two samples containing water-saturated close packing of mono-sized (100  $\mu\text{m}$ ) beads were prepared, with properties as described in Table 1. The water diffusion coefficient of these samples,  $D$ , will be close to the bulk value of water at short diffusion times, but will decrease as the diffusion time is increased. Since the two samples have similar geometry, the decrease in  $D$  will have the same time-dependence in the two samples, which results in the same diffusion behavior. However, since the beads in the two samples are composed of different materials, the relaxation properties of the two samples will be sample-dependent.

Two samples containing white oils (ExxonMobil) were also prepared, with properties as described in Table 1. The two white oils display Gaussian diffusion behavior, but have slower diffusion, and different relaxation properties compared to the systems of compact spheres.

Each of these 4 samples was prepared in 4 mm o.d. MAS-rotors. The rotors were stacked inside an ordinary 5 mm o.d. NMR tube. Measurements were then performed on each of the 4 individual samples, and on samples with two rotors stacked together, as described in Table 1.

**Table 1:** Descriptions of the different samples.

Description	$T_2$	$D$
100 $\mu\text{m}$ PS beads	1800 ms	$2 \times 10^{-9} \text{ m}^2 \text{ s}^{-1}$ (restricted)
100 $\mu\text{m}$ glass beads	60 ms	$2 \times 10^{-9} \text{ m}^2 \text{ s}^{-1}$ (restricted)
Marcol 52	315 ms	$1 \times 10^{-10} \text{ m}^2 \text{ s}^{-1}$ (non-restricted)
Marcol 152	120 ms	$2 \times 10^{-11} \text{ m}^2 \text{ s}^{-1}$ (non-restricted)
100 $\mu\text{m}$ PS beads/Marcol 52	1800 ms, 315 ms	$2 \times 10^{-9} \text{ m}^2 \text{ s}^{-1}$ (restricted), $1 \times 10^{-10} \text{ m}^2 \text{ s}^{-1}$ (non-restricted)
100 $\mu\text{m}$ glass beads/Marcol 152	60 ms, 120 ms	$2 \times 10^{-9} \text{ m}^2 \text{ s}^{-1}$ (restricted), $2 \times 10^{-11} \text{ m}^2 \text{ s}^{-1}$ (non-restricted)

Experiments were performed at 25°C on a Bruker Avance 500 MHz instrument, using a commercial probe from Bruker Biospin (DIFF30). A combined diffusion- $T_2$  ( $D$ - $T_2$ ) measurement technique with bipolar sine-shaped diffusion gradients (duration of 0.8 ms) was used [6,7]. The gradient strength was varied between 1 and 400 G/cm, while the diffusion time was varied between 2.6 and 105.6 ms. The echo spacing in the CPMG-part of the sequence was 0.2 ms, and a total of 32768 echoes were collected.

### 2.2. Analysis of data

The signal decay in the  $D$ - $T_2$  measurement can be written as a discrete sum of exponential decays for both  $D$  and  $T_2$

$$S(q, t) = \sum_{i=1}^2 p_i \exp(-4\pi^2 q^2 t_D D_i) \sum_{j=1}^2 s_j \exp(-t/T_{2,j}) \quad [1]$$

$p_i$  and  $s_i$  describe the fraction of diffusion and  $T_2$  exponential decays. The gradient wave number is  $q = \gamma g \delta / 2\pi$ , where  $\gamma$  is the gyromagnetic ratio,  $g$  and  $\delta$  are, respectively, the strength and the length of the diffusion encoding gradient pulses, and  $t_D$  is the diffusion time.

Alternatively, if we assume continuous values of  $q$  and  $t$ , and a continuous distribution of  $D$  and  $T_2$ ,  $P(D, T_2)$ , the signal can be written as

$$S(q, t) = \iint P(D, T_2) \exp(-4\pi^2 q^2 t_D D) \exp(-t/T_2) dD dT_2 \quad [2]$$

### 2.2.1 $T_2$ -filter

Eq. 1 is applied in this analysis. For each gradient wave number  $q$ ,  $T_2$ -decays are analyzed using a bi-exponential model, giving  $q$ -dependent intensities of the two  $T_2$ -components,  $s_1$  and  $s_2$ . Each of these series of intensities is analyzed as a function of  $q$  using a mono-exponential diffusion model [8]. To fulfill the second cumulant approximation [1], only gradient strengths less than 60 G/cm were used in the analysis.

### 2.2.2 $D$ -filter

Eq. 1 is applied in this analysis as well, however, unlike above, only diffusion decay of the first echo in the CPMG train is considered. At a certain  $q$ -value ( $q_c$ ) the signal from the fast diffusing component dies out, so that only the slower diffusing component contributes to the signal intensity. A mono-exponential diffusion model is used to fit the linear decay for  $q > q_c$ . The fitted signal-intensity values are then subtracted from the total decay to resolve the decay due to the faster diffusing component. The two diffusion decays are then analyzed using a mono-exponential diffusion model. To fulfill the second cumulant approximation [1], only low values ( $< 60$  G/cm) of the gradient strength were used.

### 2.2.3 Bi-exponential diffusion

Eq. 1 is applied in this analysis and then diffusion decay of the first echo in the CPMG train is analyzed using a bi-exponential diffusion model.

### 2.2.4 Two-Dimensional-Inverse Laplace Transformation

Using Eq. 2, a two-dimensional Inverse Laplace Transformation (2D-ILT) [9] is performed on the  $D$ - $T_2$  data sets. The kernel used in the inversion was  $\exp(-4\pi^2 q^2 t_D / D^{-1}) \exp(-t/T_2)$ , meaning that diffusion dimension was analyzed as a ' $T_2$ -decay', i.e.  $D^{-1}$  is the parameter determined from 2D Laplace transform. A matrix size of 32x32 was used.

### 2.2.5 Model fitting and analysis of uncertainties

The bi-exponential analysis of data was done using in-house scripts programmed in Matlab (v. R2013a) with nonlinear least-squares fitting based on the Levenberg-Marquardt Method. 2D-ILT analysis was performed using software written in Matlab [9]. The uncertainties in the discrete analysis using Eq. 1 were determined by a summation of the least-squares obtained in each separate step of the analysis. The uncertainties in the 2D-ILT results using Eq. 2 were determined from the width of the peaks in the obtained distributions.

## 3. Results and Discussion

Signals from water in PS beads and Marcol 52 have a significant difference in  $T_2$  and  $D$ . These liquid properties are representative of intra- and extra-cellular water in biological tissue in which both the  $T_2$  and  $D$  for intra- and extra-cellular water differ by approximately a factor of 10. Results presented in Fig. 1 show that when comparing measurements performed on water in close packing of PS beads alone and together with the Marcol 52 sample, the time-dependent diffusion coefficient of water is best determined using a  $T_2$ -filter [8] and a diffusion analysis that takes into account the second cumulant approximation [1]. 2D-ILT gives the most unreliable results, probably because this analysis is known to be ill-posed and more

sensitive to noise. The diffusion coefficient of Marcol 52 is fairly well determined using any of the methods. Apparently, the  $D$  of Marcol 52 increases slightly with diffusion time, but this reflects the uncertainty in the analysis, and has no physical meaning. Water fractions are best determined using the  $T_2$ -filter, although differences between the methods are not significant.

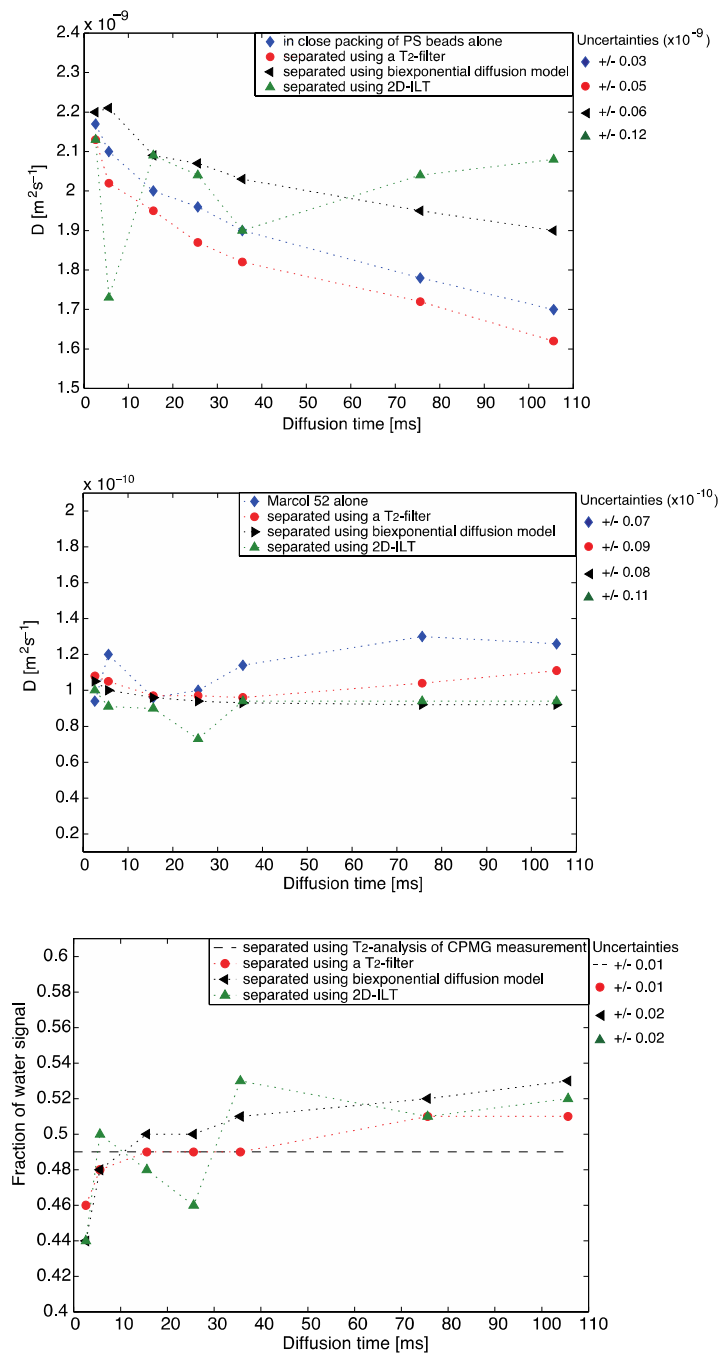


**Fig. 1:** The time-dependent diffusion coefficient of water in close packing of PS beads (top), the diffusion coefficient of Marcol 52 (middle) and the fraction of water (bottom), analysed using different models. In all the experiments the measurements on samples containing both water and Marcol 52 are compared with measurements performed on each sample alone. In the analysis of the water fraction, a bi-exponential  $T_2$ -analysis of a CPMG measurement is included for comparison.

Signals from water in glass beads and Marcol 152 have similar  $T_2$ , but large difference in  $D$ . These liquid properties are representative of a mixture of water and oil confined in a porous

rock. Fig. 2 shows that when comparing measurements performed on water in close packing of glass beads alone and together with the Marcol 152 sample, the time-dependent diffusion coefficient of water is best determined using a *D*-filter, taking into account the second cumulant approximation [1]. Again, the 2D-ILT gives the most unreliable results. The diffusion coefficient of Marcol 152 is fairly well determined using any of the methods. The fraction of water determined using a *D*-filter increases with diffusion time, which can be explained by loss of signal due to  $T_1$ -relaxation during this time interval.

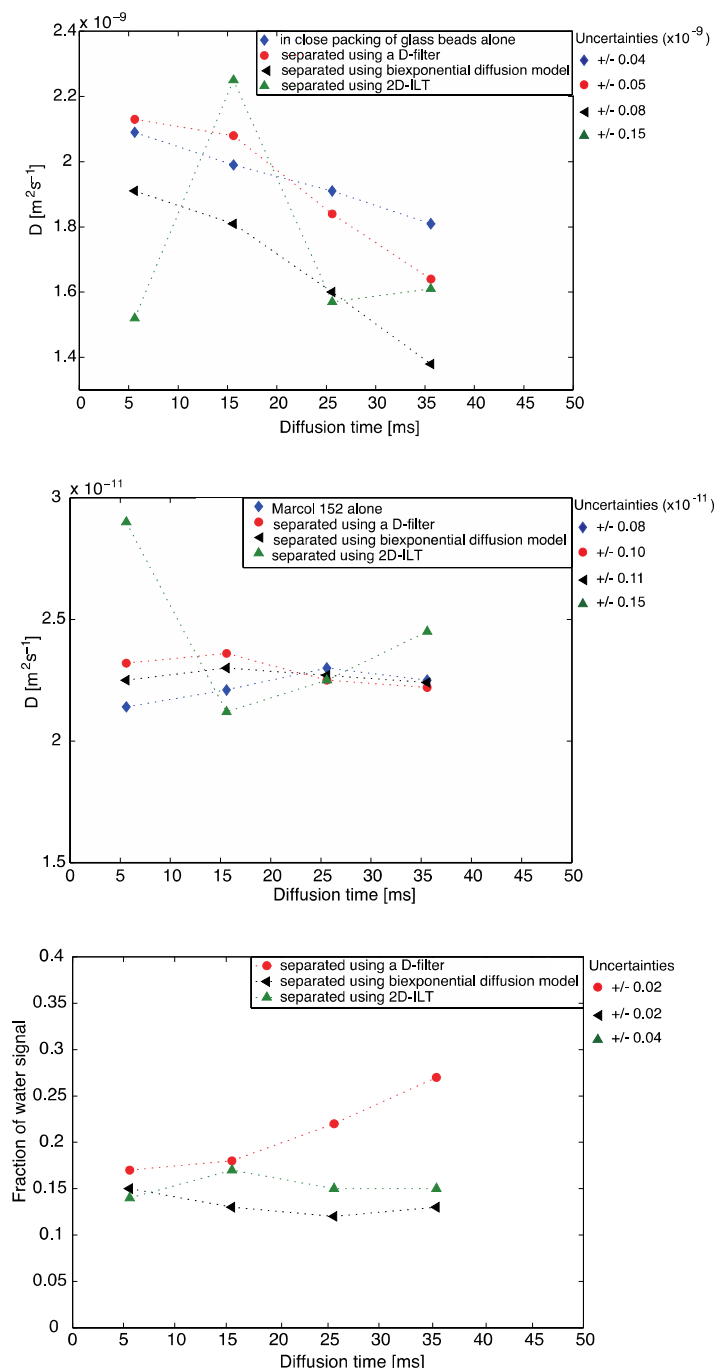


**Fig. 2:** The time-dependent diffusion coefficient of water in close packing of glass beads (top), the diffusion coefficient of Marcol 152 (middle) and the fraction of water (bottom), analysed using different models. In all the experiments the measurements on samples containing both signals from water and Marcol 152 are compared with measurements performed on each sample alone.

## 4. Conclusions

We have performed measurements in model systems where effects from restricted diffusion could be separated from effects caused by multiple diffusion coefficients.

An analysis based on multi-exponential models (bi-exponential diffusion model or 2D-Inverse Laplace Transformation) is not able to correctly accounting for effects caused by restricted diffusion in systems with multiple compartments. In contrast, analysis based on separating diffusion components due to differences in dynamics behavior prior to the diffusion analysis ( $T_2$ -filter or  $D$ -filter), combined with the second cumulant approximation [1], is more robust and more accurate in such systems.

## References

- [1] P.P. Mitra and P. N. Sen, Phys. Rev. E, 45 (1992) 143-156.
- [2] L. Wang, A. Caprihan, E. Fukushima. J Magn Reson Ser A 117 (1995) 209–219.
- [3] D. Woessner, J. Phys. Chem. 67 (1963) 1365–1367.
- [4] D.S. Grebenkov, Concepts Magn. Reson. 36A (2010) 24–35.
- [5] K.G. Helmer, B.J. Dardzinski, C.H. Sotak, NMR Biomed. (1995) 297–306.
- [6] J. G. Seland et al., Appl. Magn. Reson. 24 (2003) 41-53.
- [7] G. H. Sørland et al., Appl. Magn. Reson. 26 (2004) 417-425.
- [8] T. Pavlin et al., Proceedings of ISMRM, 16th Scientific Meeting, Toronto (2008) 287.
- [9] Provided by courtesy of Professor Paul Callaghan.